Thermo-Hydraulic Performance Evaluation, Field Synergy, and Entransy Dissipation Analysis for Hexagon-Like and Circular-Like Pin Finned Tube Bundles

En Tian, Ya-Ling He & Wen-Quan Tao

Taylor & Francis
Taylor & Francis Group

Check for updates

Thermo-Hydraulic Performance Evaluation, Field Synergy, and Entransy Dissipation Analysis for Hexagon-Like and Circular-Like Pin Finned Tube Bundles

En Tian, Ya-Ling He, and Wen-Quan Tao

Key Laboratory of Thermo-Fluid Science and Engineering, Ministry of Education, School of Energy & Power Engineering, Xi'an Jiaotong University, Xi'an, Shaanxi, China

ABSTRACT

In this paper, a comprehensive thermo-hydraulic performance evaluation for air flow across the hexagon-like and circular-like staggered pin finned tube bundle heat transfer surfaces has been numerically carried out by adopting the performance evaluation plot of enhanced heat transfer techniques oriented for energy-saving. In addition, the simulation results have also been analyzed from the viewpoints of field synergy principle and entransy dissipation extreme principle. The results indicate that the heat transfers are all enhanced based on identical pressure drop for the hexagon-like and circular-like pin finned tube bundles within the inlet velocity range from 1 m/s to 10 m/s studied. Moreover, the circular-like pin finned tube bundle offers the lowest friction factor increase ratio for the same Nusselt number increase ratio. Furthermore, the synergy between velocity and fluid temperature gradient has been proved again, having inherent consistency with the dissipation of entransy.

Introduction

Due to its simple structure and easy manufacturing, the pin fins have been used in a variety of industrial fields such as oil coolers of power transformers of electrical engineering, enhanced components of cooling devices of electronics engineering, and turbine blade cooling technique of power engineering [1–9]. Pin fins offer the most effective way of enhancing the heat transfer rate, although generally pin fins may cause higher pressure drop than other fin forms [10]. Therefore, pin fin is regarded as one of the most effective heat transfer augmentation methods through hindering the development of the thermal boundary layer [11] and shedding periodic vortex [12].

In recent years, the tubes with pin fins heat exchange surfaces have been widely employed in various engineering fields, especially in gas-side heat transfer enhancement of waste heat recovery because of its high capability of anti-deposition and anti-blockage, easy sanitation, simplicity in structure, and easiness of manufacturing. It is commonly known that the gas exhausted from many industrial systems generally contains dust particles. For other kinds of finned heat transfer surfaces, the gas-side of the heat exchange is prone to be partially blocked, and/or wore after a period of operation. But for the pin finned heat transfer surfaces such situation is much less likely to

happen. The influence on fouling (at inner and outer tube surface) on temperature and heat transfer for finned elliptical tubes has been reported in references [13, 14]. As the first stage of a serious study, in this paper only the situations with clear air of gas are simulated. The situations with dirty gas containing small particles are now underway in the authors group and will be reported later elsewhere.

A lot of researches, both numerical and experimental, have been conducted on tubes finned by pin fins. In reference [1], Nabati and Mahmoudi presented their numerical results in a heat transfer surface consisting of a rectangular duct that is fitted with different shape pin fins (circular, rectangular, and drop-shaped pin configuration) for optimizing configuration design that would maximize heat transfer rate while minimizing frictional losses in the flow. The results showed that the drop-shaped pin fin array has best heat transfer performance based on identical pressure drop. Sahiti et al. [15] showed that the heat flux from pin fin surfaces could be up to 70 times higher than the heat flux from plane surfaces. In another work, Sahiti et al. [16] also showed that despite the higher pressure drop, pin fin heat transfer surfaces perform better than all other finned surfaces. An experimental investigation was reported in reference [17] to

study the heat transfer and pressure drop characteristics of two configurations of pin finned tubes deployed in an in-line array, and the results indicated that the heat transfer for pin finned tube bundles becomes fully developed from the fifth row on, and the effect of row number for the friction factor can be negligible when the tube-row number $N > 3$. Another experiment study was presented in [18] to investigate the heat transfer characteristic of a tube with elliptic pin fins in crossflow of air by means of the heat/mass transfer analogy through the naphthalene sublimation technique, and the local heat transfer coefficients on pin fins and on the tube surface have been measured. Experimental results showed that the heat transfer coefficients of a tube with elliptic pin fins are about 30% greater than those of a smooth tube. Experimental results for condensation of steam at atmospheric pressure and low velocity on five three-dimensional pin fin tubes was reported by [19], and it was found that the enhancement of the vapor-side heat-transfer coefficient of up to 4 compared to a plain tube at the same vapor-side temperature difference. Reference [20] also reported an experimental study for condensation heat transfer of ethylene glycol at atmospheric pressure and low vapor velocity on pin fin tubes having rectangular cross section. In 2015, Tian and his coworkers [21] numerically studied the effects of six geometric parameters on the comprehensive thermo-hydraulic performance for the fully developed forced convective heat transfer on air flow across a staggered circular-pin finned tube bundle heat exchanger surface.

To the authors' knowledge, in all the studies for tubes fined with pin fin conducted in literatures the outer periphery of the pin fins is a circle as shown in Figure 1b. It is interesting to consider about the heat transfer and fluid flow characteristics if this circle periphery is changed to a hexagon-like figure as shown in Figure 1a. The heat transfer and fluid flow characteristics of these two configurations will be numerically studied in this paper. In order to have a reasonable thermo-hydraulic performance comparison for these two configurations, several comparison and analysis methods will be adopted. The general evaluation plot proposed in [22] will be used for comparing their comprehensive thermo-hydraulic performance within the oncoming velocity range from 1 m/s to 10 m/s. In [22] the authors surveyed many methods used for the comparison of performance and proposed a comprehensive comparison plot oriented for energy saving. Any enhanced structure can be represented by working points in the plot and from the location of the point under what constraint the studied structure can enhance heat transfer can be clearly identified. In addition, the results will also be analyzed from the view point of field synergy principle (FSP) [23, 24] and entransy dissipation extreme principle (EDEP) [25]. The details of these two principles are

omitted here for simplicity and the interested readers may consult the above-mentioned references.

Model description and numerical method

Physical model and computational domain

The three-dimensional governing equations of continuity, momentum, and energy for steady, incompressible fluid flow and heat transfer [26] are as follows:

Continuity equation

$$\frac{\partial u}{\partial x} + \frac{\partial v}{\partial y} + \frac{\partial w}{\partial z} = 0 \tag{1}$$

Momentum equations

$$u\frac{\partial u}{\partial x} + v\frac{\partial u}{\partial y} + w\frac{\partial u}{\partial z} = -\frac{1}{\rho}\frac{\partial p}{\partial x}$$
$$+ v\left(\frac{\partial^2 u}{\partial x^2} + \frac{\partial^2 u}{\partial y^2} + \frac{\partial^2 u}{\partial z^2}\right) \tag{2}$$

$$u\frac{\partial v}{\partial x} + v\frac{\partial v}{\partial y} + w\frac{\partial v}{\partial z} = -\frac{1}{\rho}\frac{\partial p}{\partial y}$$
$$+ v\left(\frac{\partial^2 v}{\partial x^2} + \frac{\partial^2 v}{\partial y^2} + \frac{\partial^2 v}{\partial z^2}\right) \tag{3}$$

$$u\frac{\partial w}{\partial x} + v\frac{\partial w}{\partial y} + w\frac{\partial w}{\partial z} = -\frac{1}{\rho}\frac{\partial p}{\partial z}$$
$$+ v\left(\frac{\partial^2 w}{\partial x^2} + \frac{\partial^2 w}{\partial y^2} + \frac{\partial^2 w}{\partial z^2}\right) \tag{4}$$

Energy equation

$$u\frac{\partial T}{\partial x} + v\frac{\partial T}{\partial y} + w\frac{\partial T}{\partial z} = \alpha\left(\frac{\partial^2 T}{\partial x^2} + \frac{\partial^2 T}{\partial y^2} + \frac{\partial^2 T}{\partial z^2}\right) \tag{5}$$

The governing equations are discretized by the finite volume method, the second-order upstream scheme is used for the discretization of convection term, and central scheme for the diffusion term. The linkage between velocity and pressure is dealt by SIMPLE algorithm.

From the x–y plane of the physical model of the hexagon-like and circular-like staggered pin finned tube bundle heat exchange surfaces with five tube rows presented in Figure 1, it can be seen that in spanwise direction fluid flow and heat transfer processes are periodically repeated, hence the dashed part in the figure can be selected as the numerical simulation domain in the x–y plane. Furthermore, in the z-direction the arrangement of the pin fin is also repeated from one panel of the pin fin to the next, hence only one panel of pin fin is enough. Thus the three-dimensional computation domain of the
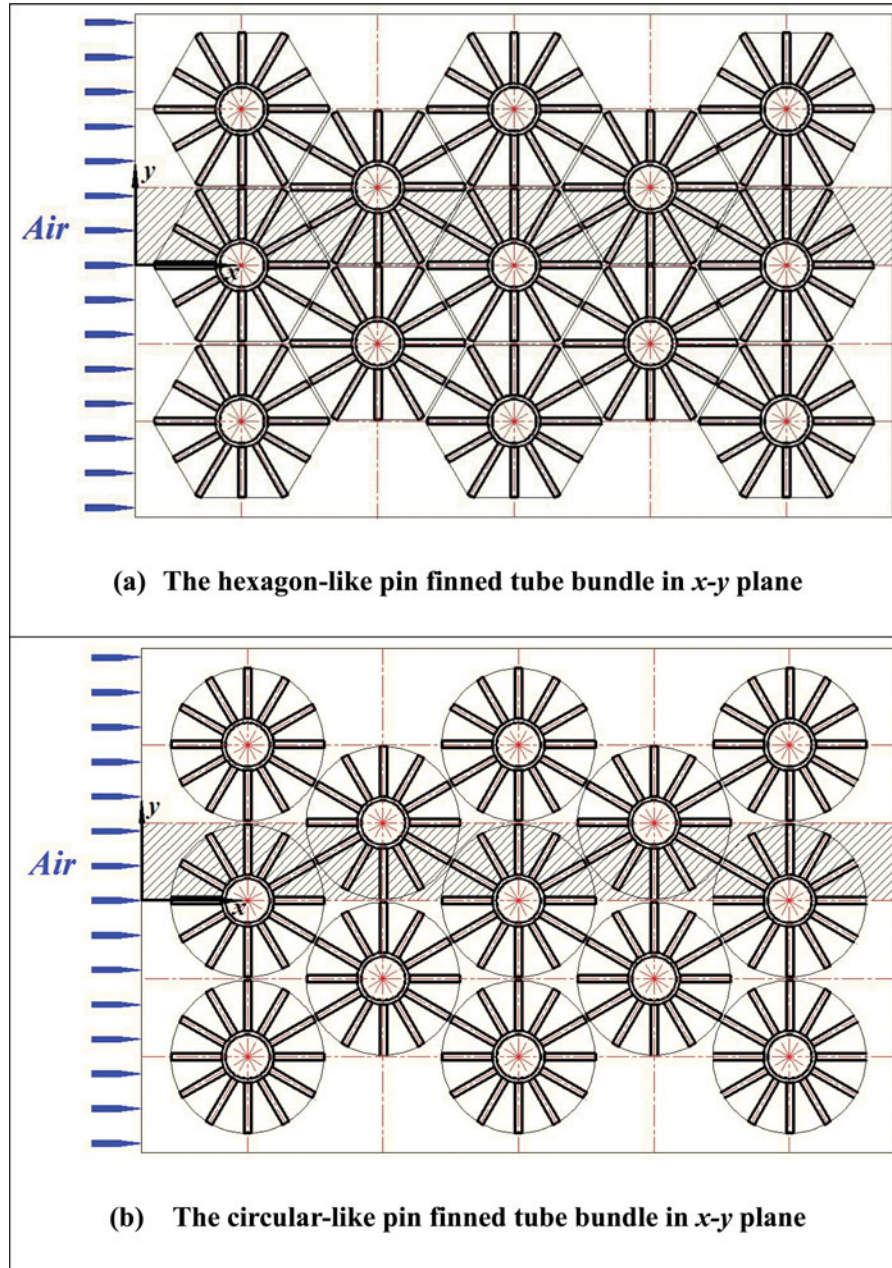
Figure 1. Physical model of two pin finned tube bundles. (a) The hexagon-like pin finned tube bundle in x–y plane. (b) The circular-like pin finned tube bundle in x–y plane.
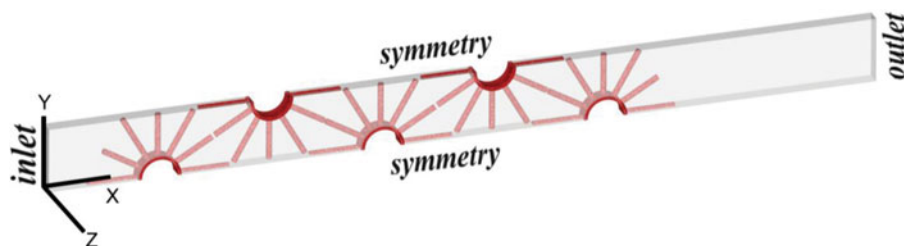
Figure 2. Computational domain of the hexagon-like pin finned tube bundle.

Table 1. Geometric Parameters.

| δ | H | | $S_{1,pf}$ | d | D | N | S_1 | S_2 |
	Hexagon-like	Circular-like						
0.0035	0.04352/0.052	0.04352	0.016	0.006	0.045	12	0.135	0.1169

Table 2. Boundary Conditions.

Inlet	Outlet	Up, down, left, right surfaces	Internal walls of tubes
Velocity Inlet	Pressure Outflow	Symmetry	$T_a = 500\,K$

hexagon-like pin finned tube bundle can be represented by Figure 2.

In this study, the flow is assumed to be incompressible, turbulent, and in steady state with constant properties. The commercial software, FLUENT 14.0, is adopted to simulate the flow and heat transfer with standard $k - \varepsilon$ turbulence model [27]. Different frontal inlet velocities (u_0) have been considered ranging from 1 m/s to 10 m/s, and the corresponding Re number ranging from 3.08×10^3 to 3.08×10^4, in which the velocity increasing step is 1 m/s. The geometric parameters adopted in the current study for the hexagon-like and circular-like pin finned tube bundles are presented in Table 1.

Boundary conditions

The boundary conditions used in the paper are illustrated in Table 2. For easier understanding readers can re-examine Figure 2; the boundary conditions of Inlet and Outlet are set to velocity inlet and pressure outlet (a standard atmospheric pressure), respectively. The inner wall of bundle tubes is set to a given temperature as 500 K. Up, down, left, and right surfaces of the domain are set to symmetry, in which up and down surfaces of the domain are perpendicular to the y axis, left and right surfaces of the domain are perpendicular to the z axis. Besides, one thing should be noted that the inner wall of bundle tube is assumed at constant temperature, meaning that the inner side heat transfer is very intensive, such as heated by water. So the temperature of the tube outside surfaces, the temperature of the pin fin surfaces and that of fluids are to be determined in the simulation process, making this problem being of conjugated type [26].
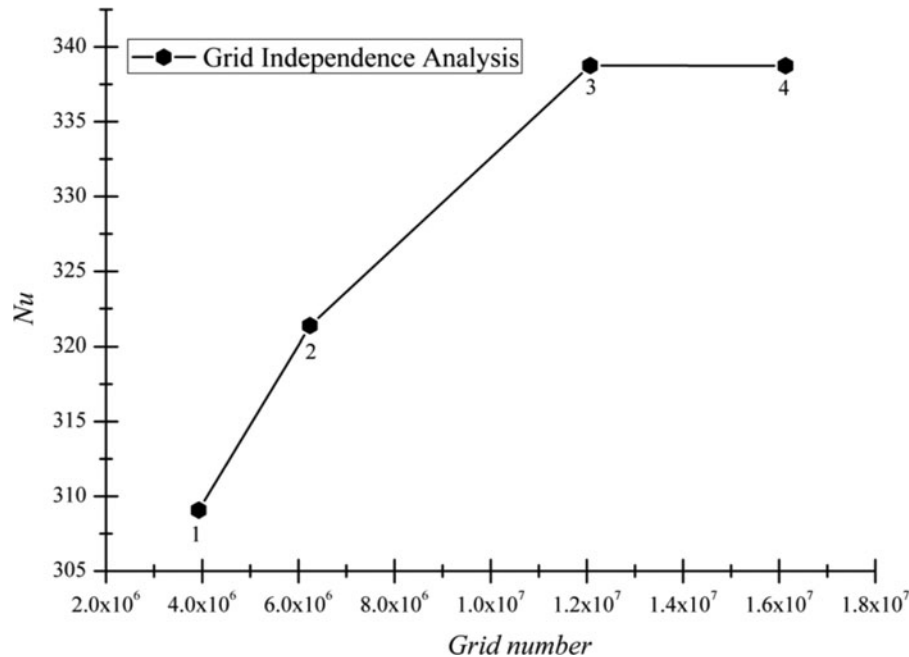
Parameter definitions

The module-averaged synergy angle of the computation domain can be obtained by using numerical integration

$$\theta_m = \arccos \frac{\sum |\overrightarrow{U}|_i \cdot |\nabla T|_i \cdot \cos\theta_i \cdot dv_i}{\sum |\overrightarrow{U}|_i \cdot |\nabla T|_i \cdot dv_i} \qquad (6)$$

Here dv_i is the volume element of the control volume.

The entransy balance formulation for convective heat transfer between a wall and a fluid is shown as below

Figure 3. Grid independence analysis.

(a) Meshes of partial solid part

(b) Meshes of partial fluid domain
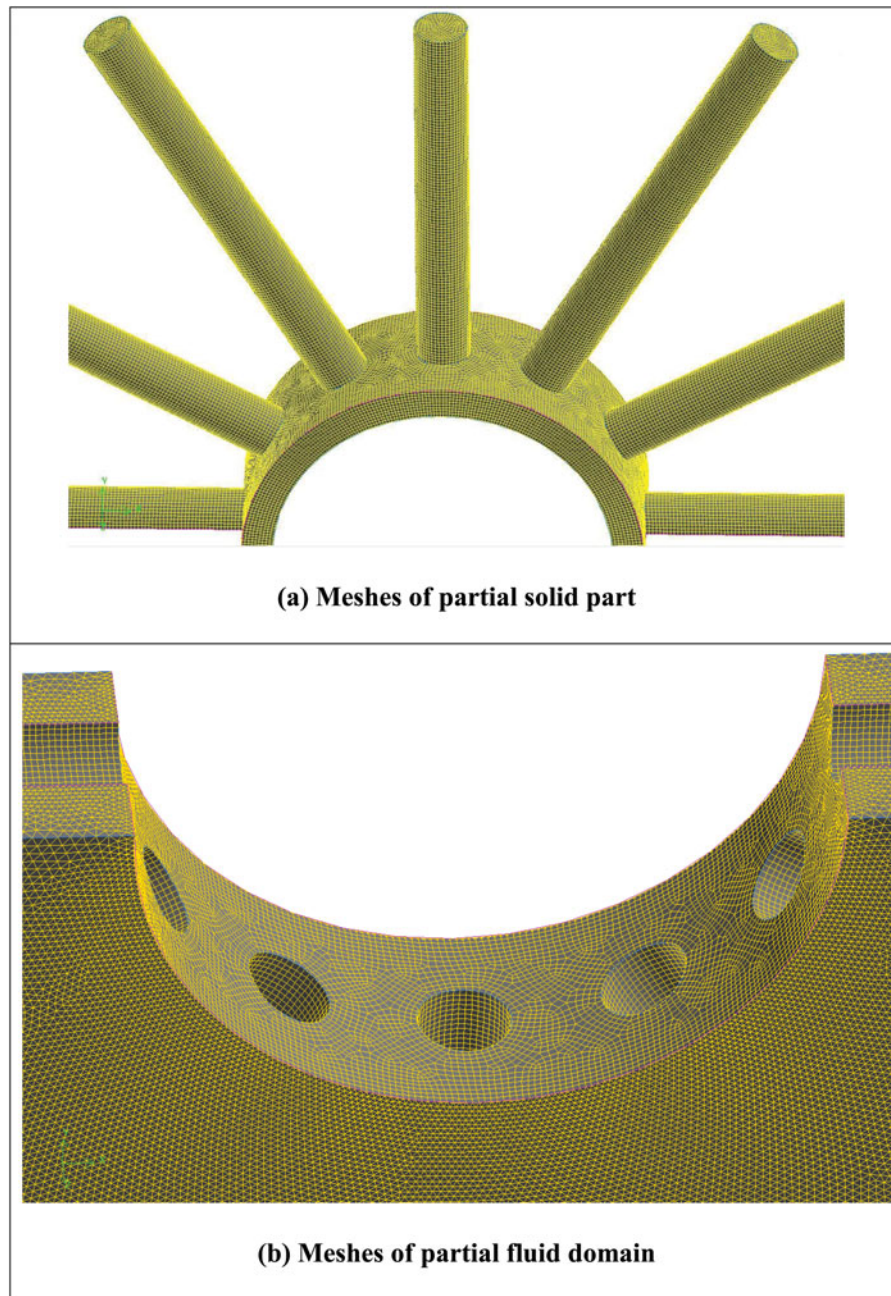
Figure 4. Meshes of hexagon-like pin finned tube bundle case. (a) Meshes of partial solid part. (b) Meshes of partial fluid domain.

(when fluid is heated):

$$\frac{1}{2}c_v q_m T_{out}^2 = \frac{1}{2}c_v q_m T_{in}^2 + c_v q_m (T_{out} - T_{in})T_a - \Delta E$$

(7)

where q_m is the mass flow rate. The term at the left hand side is the entransy flow-out carried by the fluid, while the first term at the right hand side is the entransy flow-in carried by the fluid, the second term at the right hand side is the entransy flows to the wall, and the last term is the entransy dissipated during this heat transfer process.

Grid independent analysis

For providing the grid independent solutions in the present article, four different mesh systems have been conducted with an identical frontal inlet velocity of 10 m/s. Taking the hexagon-like pin finned tube bundle as an example, the grid independence analysis is demonstrated in Figure 3. As depicted in this figure, the difference of average Nu number for the last two meshes is within 0.63%, that is to say the last mesh system can provide the mesh-independent solutions. Considering the balance between economics and
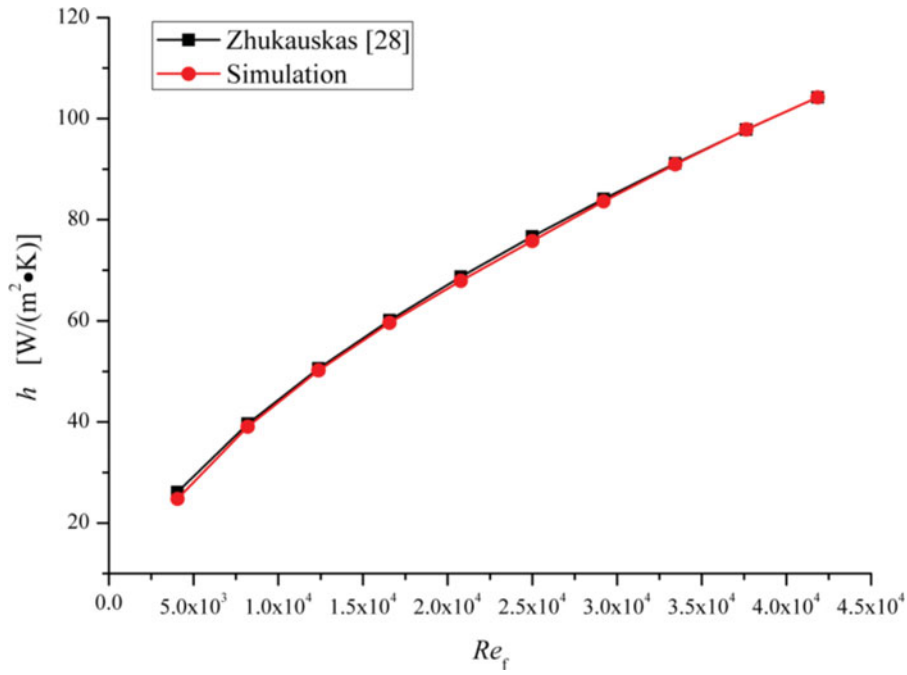
Figure 5. Comparison of simulation results with Zhukauskas correlation [28] for tube bundle without fins.

accuracy, the last but one grid system is adopted in our computation. In addition, numerical simulation results also prove that this grid system can also provide grid-independent solutions for the circular-like pin finned tube bundle.

The grid system for the hexagon-like pin finned tube bundle is shown in Figure 4. The three-dimensional grid systems used in this study are established by the commercial code GAMBIT 2.3. The fluid computational domain is discretized with unstructured tetrahedral elements, and the solid part is discretized with structured hexahedral elements.

Model validation

Zhukauskas has summarized a series of convenient empirical equations for fluid flow across tube bundle without any fins, whose reliability and feasibility has been widely validated, and the correlation adopted in this study for calculating the average Nusselt number is shown below [28, 29]:

$$Nu_f = 0.35\left(\frac{S_1}{S_2}\right)^{0.2} Re_f^{0.6} Pr_f^{0.36}(Pr_f/Pr_w)^{0.25},$$

$$\frac{S_1}{S_2} \le 2 \quad 10^3 \le Re_f \le 10^5 \tag{8}$$

(a) The temperature contour
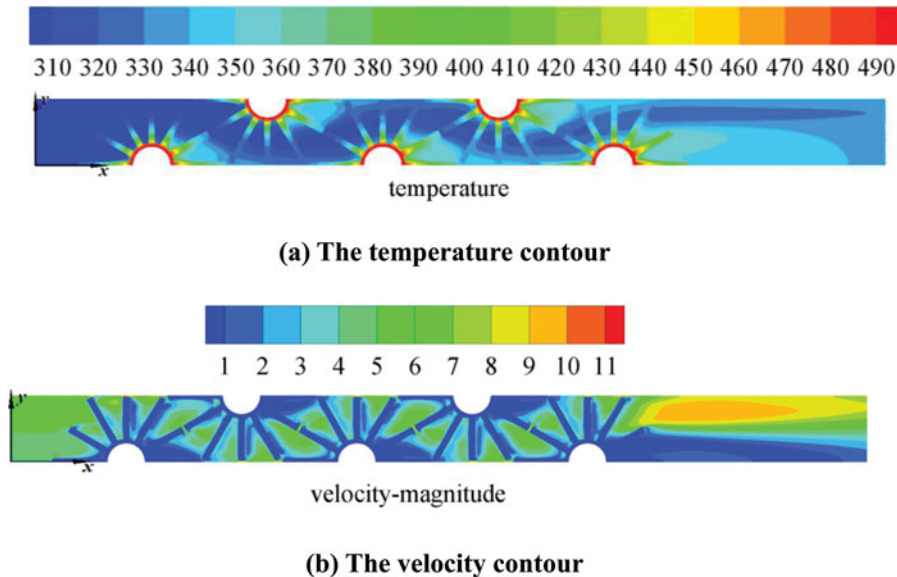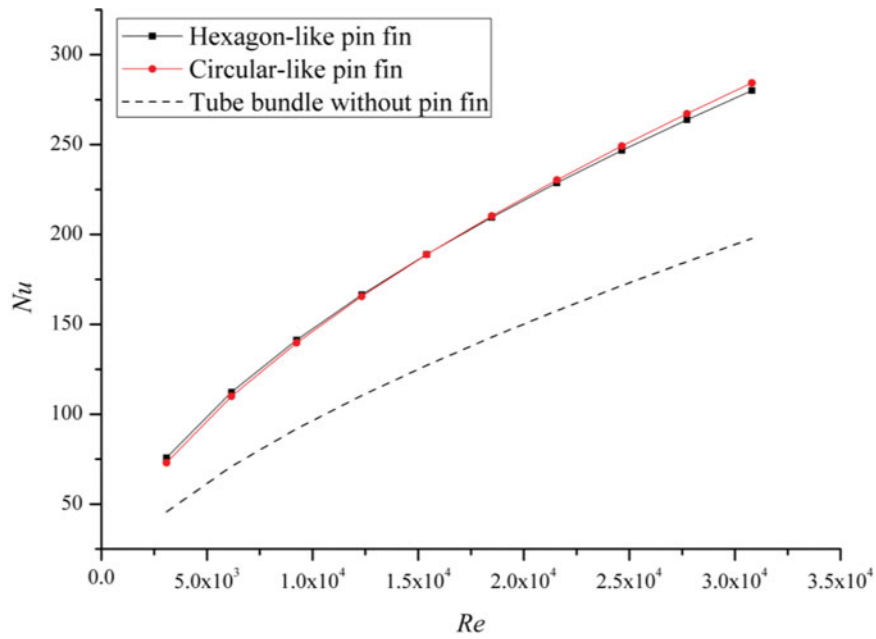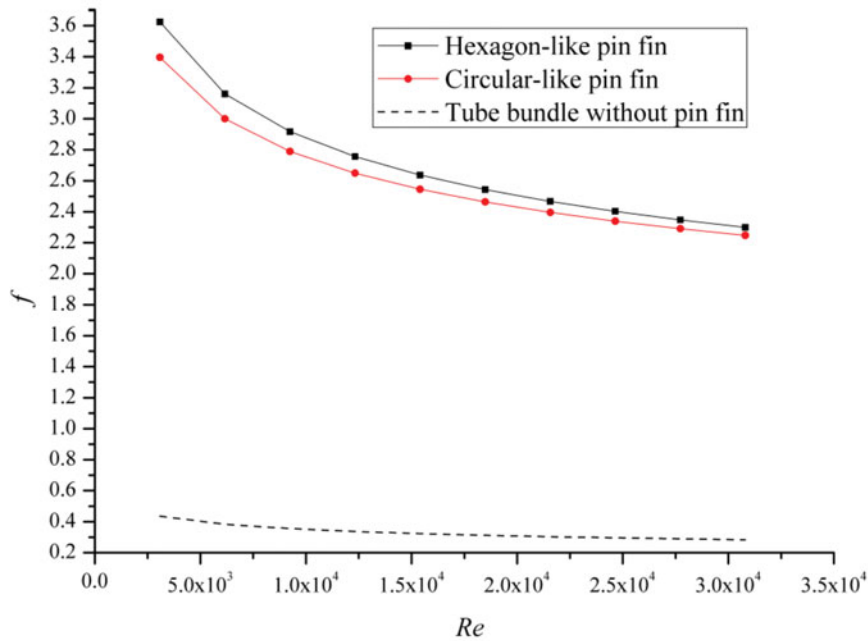

(b) The velocity contour

Figure 6. Temperature (K) and velocity contours (m/s). (a) The temperature contour. (b) The velocity contour.

(a) Nusselt number

(b) Friction factor

Figure 7. Comparisons on *Nu* and friction factor between the hexagon-like and the circular-like pin finned tube bundles. (a) Nusselt number. (b) Friction factor.

For validating the physical model and numerical methods adopted in the present paper, the staggered tube bundle without pin fins with all conditions the same is also numerical investigated. Our simulated results are compared with Zhukauskas correlation [28] shown in Figure 5. It can be easily observed that the average convective heat transfer coefficient from the simulation result and Zhukauskas correlation result are in good agreement and the average deviation is about 1.74%, indicating that the physical model and numerical methods used in the current study are reliable and accurate.
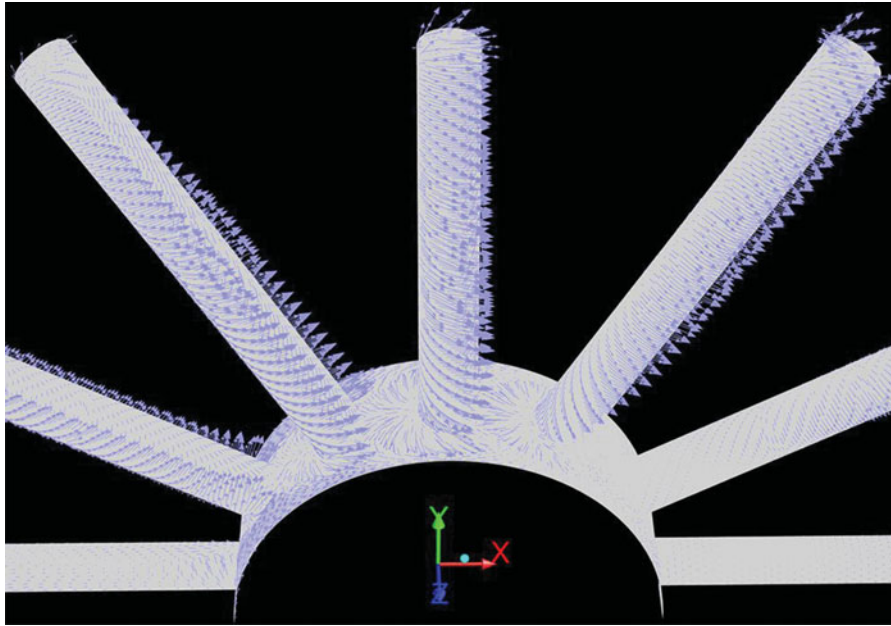
Figure 8. Velocity vectors around pin fins as inlet velocity being equal to 2 m/s for hexagon-like pin finned tube bundle (the flow direction is *x*-direction).
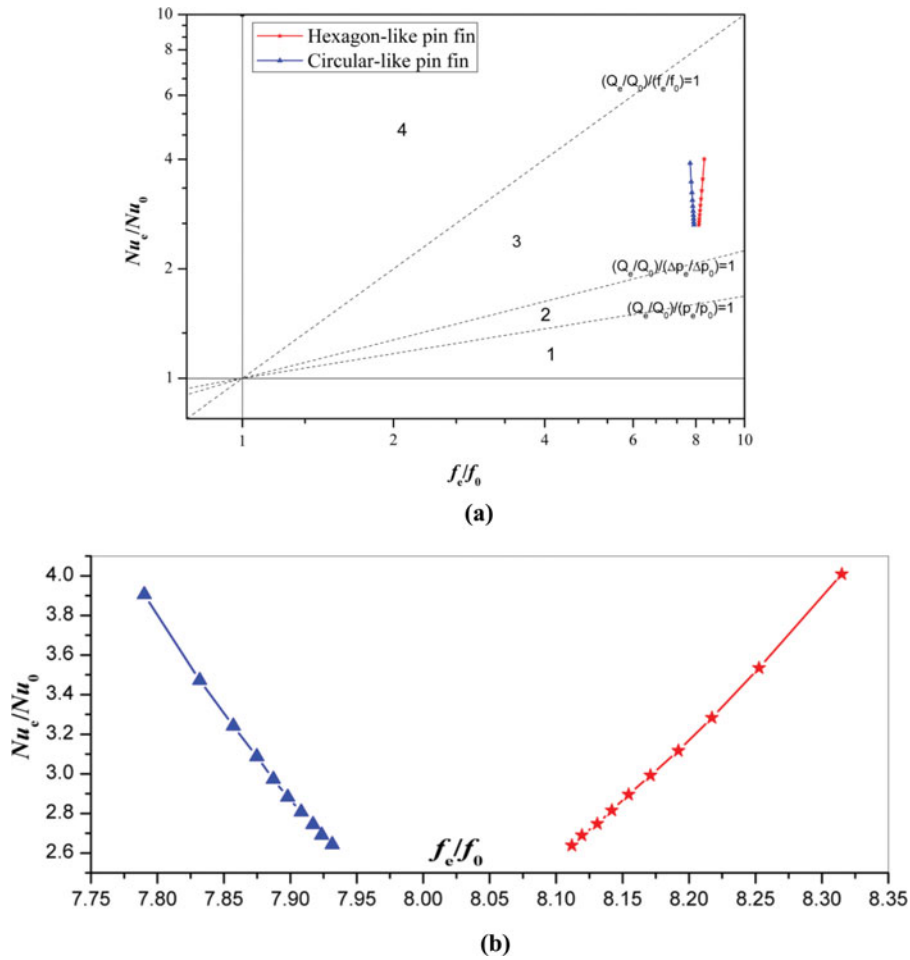
Figure 9. (a) Performance evaluation plot. (b) Zoomed region.

Figure 10. Variation of θ with Re for the hexagon-like and the circular-like pin finned tube bundles.

Results and discussion

Nusselt numbers and friction factors

The temperature and velocity contours on the x–y plane at $z = 8$ mm as $u_0 = 5$ m/s for the hexagon-like pin finned tube bundle are shown in Figure 6. The comparisons on Nusselt number Nu and friction factor f between the hexagon-like 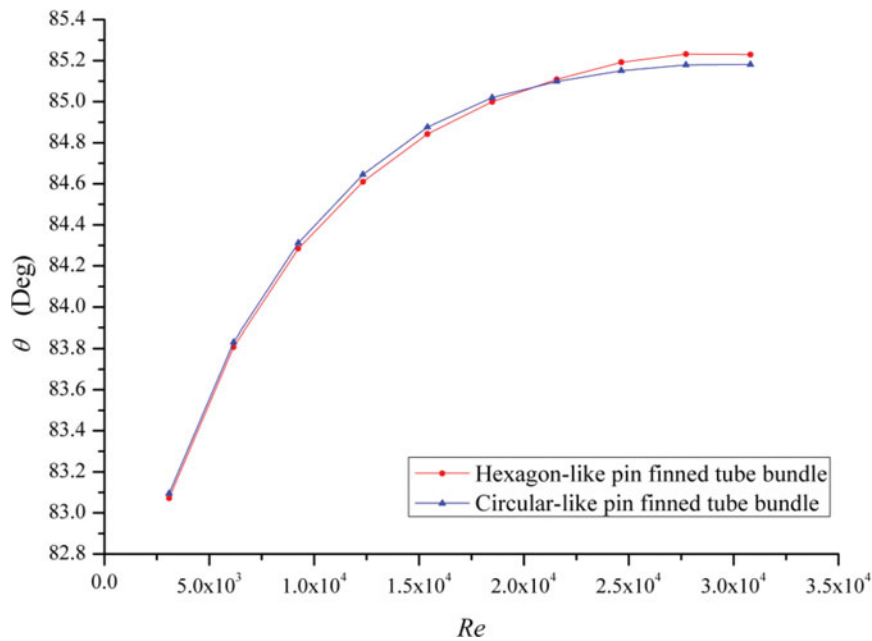and the circular-like pin finned tube bundles are shown in Figure 7. It can be found that the Nu of the hexagon-like pin finned tube bundle is slightly bigger than that of the circular-like one at lower Re number, but

the big–small relationship is switched as the increase of Re number. However the friction factor of the former is obviously bigger than that of the latter, which is very meaningful and understandable from heat transfer theory.

A three-dimensional presentation of the velocity vectors around each pin fin surface for the hexagon-like pin finned tube bundle is shown in Figure 8. It can be seen that the flow across the small pin fin is just similar to the flow across a cylinder with different attack angle, from being normal (90º) to nearly parallel (0º), and in the back of the top and bottom pin fins, small vortices can be identified.
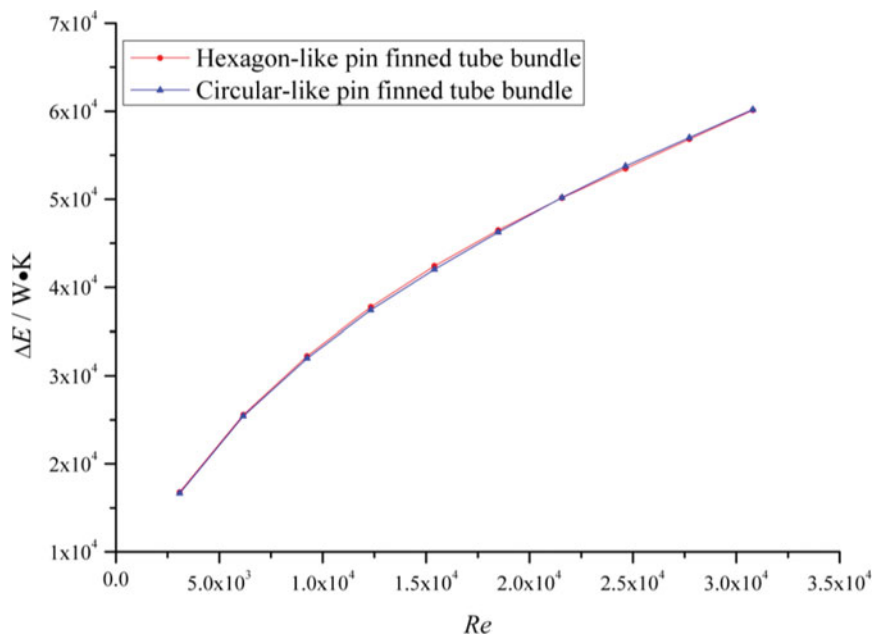
Figure 11. Entransy dissipation analysis for the hexagon-like and the circular-like pin finned tube bundles.
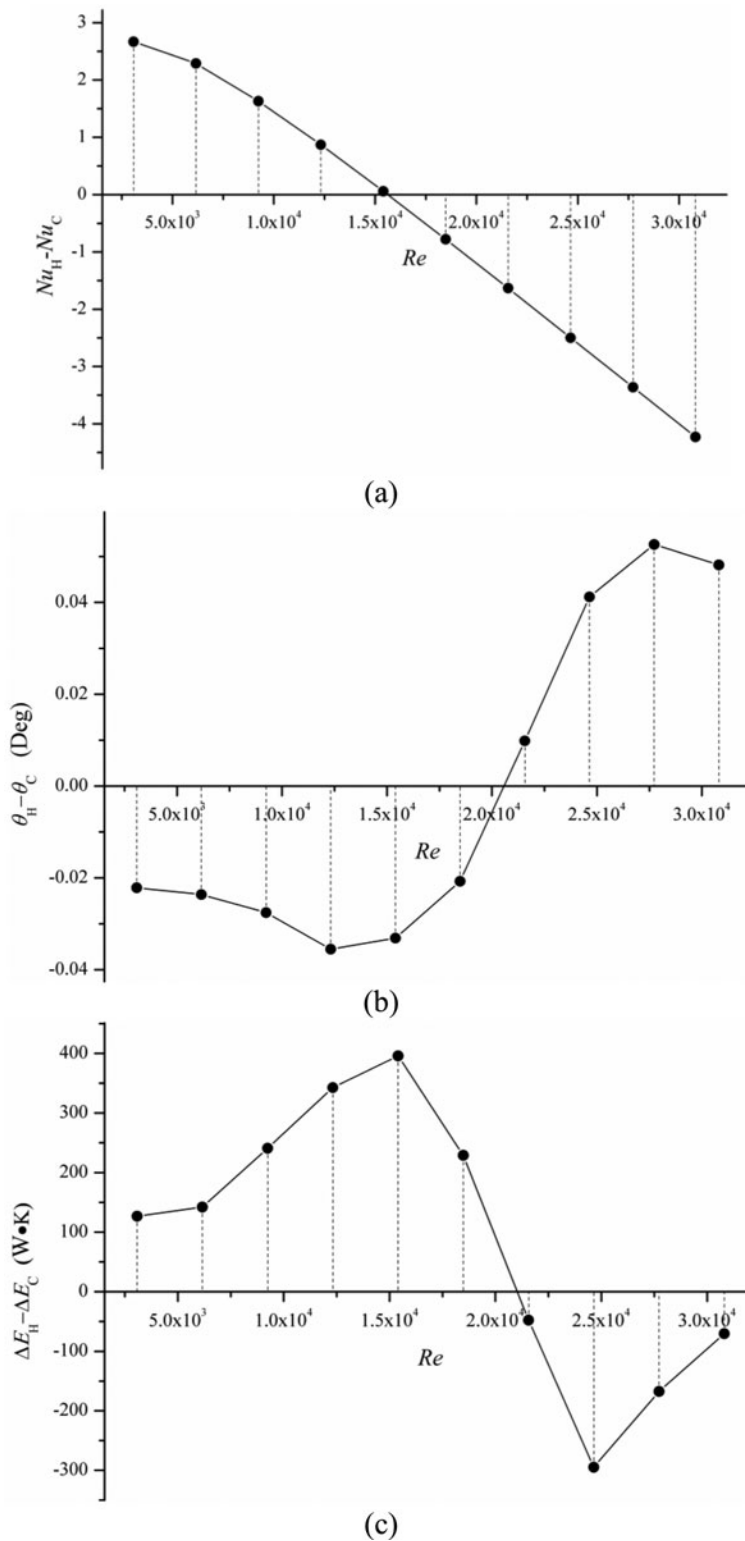
Figure 12. Differences for *Nu*, θ, ΔE between the hexagon-like and the circular-like pin finned tube bundles.

Thermo-hydraulic performance evaluation

In the thermo-hydraulic performance evaluation of enhanced heat transfer for energy-saving, as mentioned in the previous section, the reference structure is a staggered tube bundle with all conditions the same but without pin

fins. The heat transfer and flow resistance characteristics of the reference structure are also numerically simulated.

The thermo-hydraulic performance evaluation of the hexagon-like and circular-like pin finned tube bundles is depicted in Figure 9. It can be seen that the working

points are all in Region 3(Figure 9a), which means that the heat transfer is enhanced based on identical pressure drop, both for the hexagon-like and the circular-like pin finned tube bundles. Moreover, the circular-like pin finned tube bundle offers the lowest friction factor increase ratio for the same ratio of Nu_e/Nu_0 (Figure 9b). In addition, the energy-saving effectiveness of the working points are very sensitive to f_e/f_0, both for the hexagon-like and circular-like pin finned tube bundles. Furthermore, there is a very interesting observation that Nu_e/Nu_0 gets decreased but f_e/f_0 gets increased as Re number increases for the circular-like pin finned tube bundle, while for the hexagon-like pin finned tube bundle both Nu_e/Nu_0 and f_e/f_0 get decreased as Re number increases, which indicates that the energy-saving effectiveness of the hexagon-like pin finned tube bundle would be better than that of the circular-like pin finned tube bundle if the inlet velocity is much bigger than 10 m/s (corresponding Re number being much greater than 3.08×10^4).

Field synergy analysis

The simulation results are also analyzed from the view point of FSP [23, 24]. From FSP, improving synergy for the velocity vector and temperature gradient can markedly enhance heat transfer, which means that the smaller the module-averaged intersection angle, the better the heat transfer and the larger the convective heat transfer rate at the same flow rate and the same temperature difference.

The module-averaged intersection angle θ increases with the increase of Re, both for the hexagon-like and circular-like pin finned tube bundles as seen from Figure 10, which implies that the deterioration of the synergy between the temperature gradient and velocity with Re. Besides, the field synergy angle of the hexagon-like pin finned tube bundle is smaller than that of the circular-like pin finned tube bundle at lower Re number, and the big–small relationship is reversed as the increase of Re, which happens to be the opposite to the relationship of Nusselt number vs. Re between the hexagon-like and the circular-like pin finned tube bundles. The above mentioned results perfectly reveal the key points of the FSP.

Entransy dissipation extreme principle (EDEP)

From EDEP, for a given temperature condition the best heat transfer process of a fluid–solid system has the maximum dissipation of its entransy, which leads to the maximum heat transfer rate [30].

As shown in Figure 11, it can be observed that the entransy dissipation of the heat transfer process for the hexagon-like pin finned tube bundle is slightly bigger than

that for the circular-like pin finned tube bundle at lower Re number, and the big–small relationship is also switched with the increase of Re.

For better illustration of the inherent consistency between the synergy and the entransy dissipation, the differences for Nu, θ, ΔE between the hexagon-like and the circular-like pin finned tube bundles are presented in Figure 12. In [30], it was proved that the best heat transfer process should have the smallest average fluid synergy angle between the velocity and the temperature gradient at the same flow rate and the same temperature difference between fluid and wall from FSP. It was also noted that for the convective heat transfer, the FSP and the entransy dissipation extremum principle are inherently consistent. That is, the better the synergy, the larger the entransy dissipation for given temperature condition, which is aptly demonstrated by the results in this section. In other words, the result obtained in the present study is another important demonstration for the inherent consistency relationship between FSP and EDEP.

Conclusions

The Nusselt number of the hexagon-like pin finned tube bundle is slightly bigger than that of the circular-like pin finned tube bundle at lower Re number, but the big–small relationship is switched as the increase of Re number. However the friction factor of the hexagon-like pin finned tube bundle is always a bit bigger than that of the circular-like pin finned tube bundle.

For the performance evaluation of enhanced heat transfer techniques oriented for energy-saving, the heat transfers are all enhanced based on identical pressure drop for the hexagon-like and the circular-like pin finned tube bundles within the inlet velocities ranging from 1 m/s to 10 m/s studied. Moreover, the circular-like pin finned tube bundle offers the lowest friction factor increase ratio for the same ratio of Nu_e/Nu_0. In addition, the energy-saving effectiveness of the working points are very sensitive to f_e/f_0, both for the hexagon-like and circular-like pin finned tube bundles. Furthermore, the energy-saving effectiveness of the hexagon-like pin finned tube bundle would be better than that of the circular-like pin finned tube bundle if the inlet velocity is much bigger than 10 m/s (corresponding Re number being much greater than 3.08×10^4). Thus for cases with inlet velocity less than 10 m/s, the circular-like pin finned tube bundles may be used, while for cases with much higher inlet velocity the hexagon-like one is recommended.

The field synergy for the velocity vector and temperature gradient deteriorates with the increase of Re for the two type pin finned tube bundles. Synergy between velocity and fluid temperature gradient is once again

perfectly demonstrated having inherent consistency with the dissipation of entransy. That is, the best heat transfer process should have the smallest average fluid synergy angle between the velocity and the temperature gradient and the largest entransy dissipation for given temperature condition.

Acknowledgments

Nomenclature

|	
c_v	specific heat at constant volume, J/(kg• K)
D	tube diameter, m
d	circular pin fin diameter, m
EDEP	entransy dissipation extreme principle
f	friction factor
FSP	field synergy principle
h	convective heat transfer coefficient, W/(m²K)
H	pin fin length, m
k	turbulent kinetic energy
N	pin fin number around the tube periphery
Nu	Nusselt number
p	fluid pressure, Pa
Pr	Prandtl number
Q	heat transfer rate, W
q_m	mass flow rate, kg/s
Re	Reynolds number (based on u_0)
Re_f	Reynolds number (based on u_f)
S_1	transverse tube spacing, m
S_2	longitudinal tube spacing, m
$S_{1,pf}$	axial pitch of pin fins, m
T	fluid temperature, K
T_a	internal wall temperature of tubes, K
T_{in}	inlet fluid temperature, K
T_{out}	mean fluid temperature at the outlet, K
u,v,w	velocity component, m/s
$\vec{U}$	velocity vector
u_f	average velocity at the minimum cross section area, m/s
u_0	inlet fluid velocity, m/s
x,y,z	coordinate component

Greek symbols

ΔE	entransy dissipated, W• K
δ	tube thickness, m
θ	field synergy angle, Deg
∇T	temperature gradient
ρ	fluid density, kg/m³
α	proportionality coefficient in Eq. (5)
ν	fluid kinematic viscosity, m²/s
ε	turbulent dissipation rate
Δp	pressure drop, Pa

Subscripts

C	circular-like pin finned tube bundle
e	augmented surface
f	fluid
H	hexagon-like pin finned tube bundle
in	parameter at inlet
m	mean value
out	parameter at outlet
0	reference surface
w	value at the wall

Notes on contributors
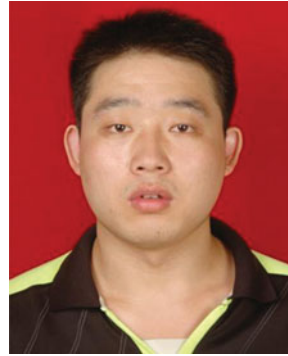
En Tian is a Ph.D. student of Xi'an Jiaotong University, Xi'an, Shaanxi, China, under the supervision of Prof. Wen-Quan Tao. He received in 2011 an undergraduate Diploma of Process Equipment and Control Engineering from Xi'an Jiaotong University. He is currently working on heat transfer enhancement for the exhausted gas and heat exchangers.

Ya-Ling He is a professor of Energy and Power Engineering at Xi'an Jiaotong University. She is also the director of the Key Laboratory of Thermo-Fluid Science and Engineering, Head of Department of Thermo-Fluid Science and Engineering, International Institute of Refrigeration – Vice President of Commission B1, associate editor of *Applied Thermal Engineering*, and associate editor of *Heat Transfer Research*. She is currently working on development and utilization of new energy (fuel cell, solar energy) and new technologies in energy storage, and multiscale simulation of heat transfer and fluid flow.

Wen-Quan Tao is a professor of Energy and Power Engineering and doctoral tutor at Xi'an Jiaotong University. He is currently the associate editor of *International Journal of Heat Mass Transfer* and *International Communications in Heat Mass Transfer*. His major research interests are heat transfer enhancement and numerical heat transfer. Recently he has been working on numerical methods for multiscale heat transfer and fluid flow problems.

References

[1] Nabati, H., and Mahmoudi, J., Numerical Study of Thermal Performance of Different Pin Fin Morphologies, *46th Conference on Simulation and Modeling* (SIMS 2005), Trondheim, Norway, 2005.

[2] Li, Q. L., Chen, Z., Flechtner, U., and Warnecke, H. J., Heat Transfer and Pressure Drop Characteristics in Rectangular Channels with Elliptic Pin Fins, *International Journal of Heat and Fluid Flow*, vol. 19, pp. 245–250, 1998.

[3] Lin, W. W., and Lee, D. J., Second-Law Analysis on a Pin Fin Array Under Crossflow, *International Journal of Heat and Mass Transfer*, vol. 40, no. 8, pp. 1937–1945, 1997.

[4] Popiel C. O., Blanch R. O., and Wojtkowiak J., Efficiency of the Horizontal Single Pin Fin Subjected to Free Convection and Radiation Heat Transfer, *Heat Transfer Engineering*, vol. 28, no. 4, pp. 299–309, 2007.

[5] Kim S. J., Kim D. K., and Oh H. H., Comparison of Fluid Flow and Thermal Characteristics of Plate-Fin and Pin Fin Heat Sinks Subject to a Parallel Flow, *Heat Transfer Engineering*, vol. 29, no. 2, pp. 169–177, 2008.

[6] Xue Y. F., Yuan M. Z., Ma A. X., and Wei J. J., Enhanced Boiling Heat Transfer by Using Micro-Pin Finned Surface in Three Different Test Systems, *Heat Transfer Engineering*, vol. 32, pp. 1062–1068, 2011.

[7] Tu J. P., Yuen W. W., and Gong Y. S., An Assessment of Direct Chip Cooling Enhancement Using Pin Fins, *Heat Transfer Engineering*, vol. 33, no. 10, pp. 845–852, 2012.

[8] Zhang Y. H., Wei J. J., Kong X., and Guo L., Confined Submerged Jet Impingement Boiling of Subcooled FC-72 over Micro-Pin Finned Surfaces, *Heat Transfer Engineering*, vol. 37, pp. 269–278, 2016.

[9] Rasouli E., and Narayanan V., Single-Phase Cryogenic Flow and Heat Transfer Through Microscale Pin Fin Heat Sinks, *Heat Transfer Engineering*, vol. 37, no. 11, pp. 994–1011, 2016.

[10] Sahiti, N., Lemouedda, A., Stojkovic, D., Durst, F., and Franz, E., Performance Comparison of Pin Fin In-Duct Flow Arrays with Various Pin Cross-Sections, *Applied Thermal Engineering*, vol. 26, pp. 1176–1192, 2006.

[11] Zhou, F., and Catton, I., Numerical Evaluation of Flow and Heat Transfer in Plate-Pin Fin Heat Sinks with Various Pin Cross-Sections, *Numerical Heat Transfer, Part A: Application*, vol. 60, pp. 107–128, 2011.

[12] Yang, K. S., Chu, W. H., Chen, I. Y., and Wang, C. C., A Comparative Study of the Airside Performance of Heat Sinks, *International Journal of Heat and Mass Transfer*, vol. 50, pp. 4661–4667, 2007.

[13] Łopata, S., and Ocłoń, P., Numerical Study of the Effect of Fouling on Local Heat Transfer Conditions in a High-Temperature Fin-and-Tube Heat Exchanger, *Energy*, vol. 92, pp. 100–116, 2015.

[14] Ocłoń, P., Łopata, S., Nowak, M., and Benim, A.C., Numerical Study on the Effect of Inner Tube Fouling on the Thermal Performance of High-Temperature Fin-and-Tube Heat Exchanger, *Progress in Computational Fluid Dynamics*, vol. 15, no. 5, pp. 290–306, 2015.

[15] Sahiti, N., Durst, F., and Dewan, A., Heat Transfer Enhancement by Pin Elements, *International Journal of Heat and Mass Transfer*, vol. 48, pp. 4738–4747, 2005.

[16] Sahiti, N., Durst, F., and Dewan, A., Strategy for Selection of Elements for Heat Transfer Enhancement, *International Journal of Heat and Mass Transfer*, vol. 49, pp. 3392–3400, 2006.

[17] Yao, S. G., and Zhu, D. S., Experimental Research on Heat Transfer and Pressure Drop of Two Configurations of Pin Finned-Tubes in an In-line Array, *Journal of Thermal Science*, vol. 3, no. 3, pp. 167–172, 1994.

[18] Li, Q. L., Ma, L. X., Chen, Z., and Warnecke H. J., Heat Transfer Characteristics of a Tube with Elliptic Pin Fins in Crossflow of Air, *Heat and Mass Transfer*, vol. 39, pp. 529–533, 2003.

[19] Baisar, M., and Briggs, A., Condensation of Steam on Pin Fin Tubes: Effect of Circumferential Pin Thickness and Spacing, *Heat Transfer Engineering*, vol. 30, no. 13, pp. 1017–1023, 2009.

[20] Ali, H. M., and Briggs, A., Enhanced Condensation of Ethylene Glycol on Single Pin Fin Tubes: Effect of Pin Geometry, Trans. ASME *Journal of Heat Transfer*, vol. 134, pp. 011503-1–011503-8, 2012.

[21] Tian, E., He, Y. L., and Tao, W. Q., Numerical Simulation of Airflow Across Staggered Circular-Pin Finned Tube Bundle, *Numerical Heat Transfer*, vol. 68, pp. 737–760, 2015.

[22] Fan, J. F., Ding, W. K., He, Y. L., and Tao, W. Q., A Performance Evaluation Plot of Enhanced Heat Transfer Techniques Oriented for Energy-Saving, *International Journal of Heat and Mass Transfer*, vol. 52, pp. 33–44, 2009.

[23] Guo, Z.Y., Li, D.Y., and Wang, B. X., A Novel Concept for Convective Heat Transfer Enhancement, *International Journal of Heat and Mass Transfer*, vol. 41, pp. 2221–2225, 1998.

[24] Tao, W. Q., Guo, Z. Y., and Wang, B. X., Field Synergy Principle for Enhancing Convective Heat Transfer – Its Extension and Numerical Verifications, *International Journal of Heat and Mass Transfer*, vol. 45, pp. 3849–3856, 2002.

[25] Guo, Z. Y., Zhu, H. Y., and Liang, X. G., Entransy—a Physical Quantity Describing Heat Transfer Ability, *International Journal of Heat and Mass Transfer*, vol. 50, pp. 2545–2556, 2007.

[26] Tao, W. Q., *Numerical Heat Transfer*, 2nd ed., Xi'an Jiaotong University Press, Xi'an, 2001.

[27] Jongen, T., Simulation and Modeling of Turbulent Incompressible Flows. Ph.D. thesis. EPF Lausanne, Lausanne, Switzerland, 1992.

[28] Zukauskas A. A., Heat Transfer from Tubes in Cross Flow, *Advances in Heat Transfer*, vol. 8, pp. 93–160, 1972.

[29] Yang S. M., and Tao W. Q., *Heat Transfer*, 4th ed., Higher Education Press, Beijing, 2006.

[30] He, Y. L., and Tao, W. Q., Numerical Studies on the Inherent Interrelationship Between Field Synergy Principle and Entransy Dissipation Extreme Principle for Enhancing Convective Heat Transfer, *International Journal of Heat and Mass Transfer*, vol. 74, pp. 196–205, 2014.